

Exceptionally fast ejecta seen in light echoes of Eta Carinae’s Great Eruption

Nathan Smith^{1*}, Armin Rest^{2,3}, Jennifer E. Andrews¹, Tom Matheson⁴,
 Federica B. Bianco^{5,6}, Jose L. Prieto^{7,8}, David J. James⁹, R. Chris Smith¹⁰,
 Giovanni Maria Strampelli^{2,11}, and A. Zenteno¹⁰

¹ *Steward Observatory, University of Arizona, 933 N. Cherry Ave., Tucson, AZ 85721, USA*

² *Space Telescope Science Institute, 3700 San Martin Drive, Baltimore, MD 21218, USA*

³ *Department of Physics and Astronomy, The Johns Hopkins University, 3400 North Charles Street, Baltimore, MD 21218, USA*

⁴ *National Optical Astronomy Observatory, Tucson, AZ 85719, USA*

⁵ *CCPP, New York University, 4 Washington Place, New York, NY 10003, USA*

⁶ *Center for Urban Science and Progress, New York University, 1 MetroTech Center, Brooklyn, NY 11201, USA*

⁷ *Núcleo de Astronomia de la Facultad de Ingeniería, Universidad Diego Portales, Av. Ejercito 441, Santiago, Chile*

⁸ *Millennium Institute of Astrophysics, Santiago, Chile*

⁹ *Event Horizon Telescope, Smithsonian Astrophysical Observatory MS 42, Harvard-Smithsonian Center for Astrophysics, 60 Garden Street, Cambridge, MA 02138, USA*

¹⁰ *Cerro Tololo Inter-American Observatory, National Optical Astronomy Observatory, Colina El Pino S/N, La Serena, Chile*

¹¹ *Universidad de La Laguna, Tenerife, Spain*

6 August 2018

ABSTRACT

In our ongoing study of η Carinae’s light echoes, there is a relatively bright echo that has been fading slowly, reflecting the 1845–1858 plateau phase of the eruption. A separate paper discusses its detailed evolution, but here we highlight one important result: the H α line in this echo shows extremely broad emission wings that reach $-10,000$ km s⁻¹ to the blue and $+20,000$ km s⁻¹ to the red. The line profile shape is inconsistent with electron scattering wings, so the broad wings indicate high-velocity outflowing material. To our knowledge, these are the fastest outflow speeds ever seen in a non-terminal massive star eruption. The broad wings are absent in early phases of the eruption in the 1840s, but strengthen in the 1850s. These speeds are two orders of magnitude faster than the escape speed from a warm supergiant, and 5–10 times faster than winds from O-type or Wolf-Rayet stars. Instead, they are reminiscent of fast supernova ejecta or outflows from accreting compact objects, profoundly impacting our understanding of η Car and related transients. This echo views η Car from latitudes near the equator, so the high speed does not trace a collimated polar jet aligned with the Homunculus. Combined with fast material in the Outer Ejecta, it indicates a wide-angle explosive outflow. The fast material may constitute a small fraction of the total outflowing mass, most of which expands at ~ 600 km s⁻¹. This is reminiscent of fast material revealed by broad absorption during the presupernova eruptions of SN 2009ip.

Key words: circumstellar matter — stars: evolution — stars: winds, outflows

1 INTRODUCTION

The massive evolved star η Carinae serves as a tremendous reservoir of information about episodic mass loss in the late-stage evolution of massive stars. It is uniquely valuable because it is nearby, because it underwent a spectacular “Great

Eruption” event observed in the mid-19th century, and because we can now observe the spatially resolved shrapnel of that event with modern tools like the *Hubble Space Telescope* (*HST*). Added to this list is the recent discovery of light echoes from the 19th century eruption (Rest et al. 2012), which now allow us to obtain spectra of light from an event that was seen directly by Earth-based observers before the invention of the astronomical spectrograph. This is similar

* E-mail: nathans@as.arizona.edu

to studies of light echoes from historical supernovae (SNe) and SN remnants in the Milky Way and Large Magellanic Cloud (Rest et al. 2005a,b, 2008).

Spectroscopy of these light echoes provides informative comparisons between η Car and extragalactic eruptions. Based mostly on its historical light curve (Smith & Frew 2011), η Car has been a prototype for understanding luminous blue variable (LBV) giant eruptions and SN impostors (Smith et al. 2011; Van Dyk & Matheson 2012). Eruptions akin to η Car have been discussed in the context of brief precursor episodes of extreme mass loss that create circumstellar material (CSM) of super-luminous Type IIn supernovae (Smith et al. 2007; Smith & McCray 2007). In addition to extreme η Car-like mass loss, several lines of evidence connect LBVs and SNe with dense CSM (see Smith 2014 for a review; also e.g., Gal-Yam & Leonard 2009; Groh et al. 2013; Groh 2014; Justham et al. 2014; Kotak & Vink 2006; Mauerhan et al. 2013; Smith & Owocki 2006; Smith 2007; Smith et al. 2008, 2011; Trundle et al. 2008). LBVs have the highest known mass-loss rates of any stars before death, where LBV giant eruptions can lose as much as several M_{\odot} in a few years (see Smith 2014).

The physical trigger and mechanism of these LBV-like giant eruptions are still highly uncertain. Eruptive mass loss is usually discussed in the context of super-Eddington winds (Davidson 1987; Owocki & Gayley 1997; Owocki et al. 2004; Owocki & Shaviv 2016; Quataert et al. 2016; Smith & Owocki 2006; van Marle et al. 2008). This framework addresses how mass can be lost at such a high rate, but it does not account for where the extra energy comes from. There are also (sometimes overlapping) scenarios that have been discussed, involving binary mergers, stellar collisions, violent common envelope events, accretion events onto a companion (perhaps including compact object companions, although this has not been discussed much for η Car), violent pulsations, extreme magnetic activity, pulsational pair instability eruptions, unsteady or explosive nuclear burning, and wave driving associated with late nuclear burning phases approaching core collapse (Gallagher 1989; Fuller 2017; Guzik & Lovekin 2012; Harpaz & Soker 2009; Kashi & Soker 2009; Portegies Zwart & van den Heuvel 2016; Piro 2011; Quataert & Shiode 2012; Shiode & Quataert 2014; Smith 2011; Smith & Arnett 2014; Smith et al. 2011, 2016b; Soker 2001, 2004; Woosley 2017). In any case, a tremendous amount of mass (several M_{\odot}) leaves the star in a brief window of time (a few years), and observational constraints on the outflow properties provide a key way to guide theoretical interpretation.

In general, quasi-steady radiation-driven winds are expected to leave a star with a speed that is within a factor of order unity compared to the escape speed from the star's surface. That is why red supergiant winds are slow (10s of km s^{-1}), blue supergiant winds are a few hundred km s^{-1} , O-type stars have winds around 1000 km s^{-1} , and more compact H-poor Wolf-Rayet star winds are $2000\text{--}3000 \text{ km s}^{-1}$ (see Smith 2014 for a review). For example, line-driven winds of hot O-type stars have a ratio of their terminal wind to the star's escape speed of $v_{\infty}/v_{\text{esc}} \approx 2.6$, and cooler stars below about $21,000 \text{ K}$ have $v_{\infty}/v_{\text{esc}} \approx 1.3$ (Lamers et al. 1995; Vink et al. 1999). Line driven wind theory and observations indicate that $v_{\infty}/v_{\text{esc}} \approx 2.6$ is expected to become lower as

the star's temperature drops (Castor, Abbott & Klein 1975; Abbott 1982; Pauldrach et al. 1986; Pauldrach & Puls 1990; Lamers et al. 1995; Vink et al. 1999). For a strongly super-Eddington wind in an LBV, where Γ substantially exceeds 1, the effective gravity is low, the stellar envelope may inflate, the wind may show a complicated pattern of outflow and infall, and material may ultimately leak out slowly. The atmosphere may be porous (Owocki et al. 2004), perhaps leading to a range of outflow speeds, but we don't expect a steady wind-driven outflow with a high mass-loss rate to be many times faster than a star's escape speed (Owocki et al. 2004; van Marle et al. 2008; Owocki et al. 2017). Numerical simulations of super-Eddington continuum-driven winds predict terminal wind speeds below the star's surface escape speed (van Marle et al. 2008, 2009).

Observationally, a wide range of outflow speeds are seen in the η Car system. The bulk outflow of the present-day wind is around $400\text{--}500 \text{ km s}^{-1}$ (Hillier et al. 2006), although with some faster speeds up to around 1000 km s^{-1} in the polar wind (Smith et al. 2003a). The bipolar Homunculus nebula, which contains most of the mass ejected in the 19th century eruption (Morse et al. 2001; Smith 2017) has a range of speeds that vary with latitude from 650 km s^{-1} at the poles to about 50 km s^{-1} in the pinched waist at the equator (Smith 2006). However, there is also faster material in the system. Hard X-ray emission from the colliding-wind binary suggests that a companion star has a very fast wind of $2000\text{--}3000 \text{ km s}^{-1}$ (Corcoran et al. 2001; Pittard & Corcoran 2002; Parkin et al. 2011; Russell et al. 2016). In spectra of the central star system, speeds as fast as $\sim 2000 \text{ km s}^{-1}$ are only seen in absorption at certain phases, attributed to the companion's wind shocking the primary star's wind along our line of sight (Groh et al. 2010).

So far, the fastest material associated with η Car has been seen in the Outer Ejecta, where filaments have speeds based on Doppler shifts and projection angles as high as 5000 km s^{-1} (Smith 2008). (Most of the Outer Ejecta seen in images are slower, moving at a few hundred km s^{-1} ; Kiminki et al. 2016; Weis 2012.) This fast material, combined with the high ratio of kinetic energy to total radiated energy in the eruption (Smith et al. 2003b), has led to speculation that the Great Eruption may have been partly caused by a hydrodynamic explosion (Smith 2006, 2008, 2013). Spectra of η Car's light echoes (Rest et al. 2012; Prieto et al. 2014) also seemed inconsistent with traditional expectations for a simple wind pseudo-photosphere (Davidson 1987), although Owocki & Shaviv (2016) showed that proper treatment of opacity and radiative equilibrium in such a wind may lead to cool temperatures around 5000 K . Well-developed models for sub-energetic and non-terminal explosive events do not yet exist, but an explosive ejection of material and a surviving star might arise if energy is deposited in the star's envelope that is less than the total binding energy of the core, but enough to unbind the outer layers. Dessart et al. (2010) explored how stellar envelopes might respond to such energy deposition, and found some cases with partial envelope ejection and model light curves reminiscent of SN impostors. Ro & Matzner (2017) argued that any deep energy deposition at a rate that substantially exceeds the steady luminosity of the star is likely to steepen to a shock. For the specific case of η Car's eruption, Smith (2013) argued that an explosive ejection of fast

Table 1. Optical Spectroscopy of Light Echo EC2

UT Date	Tel./Intr.	grating	$\Delta\lambda$ (Å)	slit	PA
2014 Nov 03	Gemini/GMOS	R400	5000-9200	1''0	293°
2015 Jan 20	Baade/IMACS f4	1200	5500-7200	0''7	293°
2015 Jan 20	Baade/IMACS f4	300	4000-9000	0''7	293°

material interacting with a previous slow wind could account for the historical light curve and several properties of the Homunculus, where CSM interaction leads to efficient radiative cooling as in SNe IIn.

In this paper, we present evidence based on Doppler shifts in light echo spectra from the Great Eruption, which show that there was in fact an explosive ejection of very fast material relatively late in the eruption. The observed speeds in excess of $10,000 \text{ km s}^{-1}$ suggest that a small fraction of the mass was accelerated to very high speeds by a blast wave, confirming similar conclusions based on fast nebular ejecta observed around the star at the present epoch (Smith 2008, 2013).

2 OPTICAL SPECTROSCOPY

Following the discovery of light echoes from η Carinae (Rest et al. 2012), we have continued to follow the slow spectral evolution of several echoes. So far in previous papers, we have discussed the initial spectra and spectral evolution of a close group of echoes (called “EC1”) thought to arise from pre-1845 peaks in the light curve (Rest et al. 2012; Prieto et al. 2014), but we have monitored a number of other echo systems as well.

One echo, which we refer to henceforth as “EC2”, captured our attention because it was relatively bright in our first-epoch image in 2003, and has faded very slowly over several years since then. EC2 arises from the reflection off of a cometary shaped dust cloud. We infer from its slow rate of fading that EC2 reflects light from the main plateau of the Great Eruption in 1845-1858; this is explained in more detail in our companion paper (Smith et al. 2018 S18 hereafter), where we analyze the imaging photometry of the echo. Based on the probable time delay of about 160 yr, spectra that we have been obtaining in the last few years trace light emitted by η Car in its mid-1850s plateau. From the known geometry of light echo paraboloids (Couderc 1939) and with a known time delay, one can deduce the viewing angle for any echo. EC2’s position on the sky is near the EC1 echoes discussed previously by Rest et al. (2012) and Prieto et al. (2014). Like those echoes, EC2 views η Car from a vantage point that is near the equatorial plane of the Homunculus (within $\sim 10^\circ$), with the uncertainty dominated by the value of the adopted time delay of the echo. The fact that this viewing angle is near the equator and not the polar axis is an important detail, to which we return later.

The full photometric and spectroscopic evolution of EC2 will be described in detail in a more lengthy paper referenced above (S18). Here we focus on just one aspect of these data that stands out as an important and independent result. Briefly, EC2 spectra show faint but extremely broad line wings that indicate faster ejecta than has ever been seen before in η Car or in any other massive star eruption. The

result described below was quite astonishing to us, and profoundly impacts our understanding of the nature of η Car’s eruption. Implications are discussed in the next section.

We obtained low- and moderate-resolution spectra of the EC2 echo on a number of dates from 2011 to the present, but we only mention a few of those in this paper. We obtained one spectrum on 2014 Nov 13 using the Gemini Multi-Object Spectrograph (GMOS) (Hook et al. 2002) at Gemini South on Cerro Pachón. Nod-and-shuffle techniques (Glazebrook & Bland-Hawthorn 2001) were used with GMOS to improve sky subtraction. Standard CCD processing and spectrum extraction were accomplished with IRAF¹. The spectrum covers the range $4540 - 9250 \text{ \AA}$ with a resolution of $\sim 9 \text{ \AA}$. We used an optimized version² of the LA Cosmic algorithm (van Dokkum 2001) to eliminate cosmic rays. We optimally extracted the spectrum using the algorithm of Horne (1986). Low-order polynomial fits to calibration-lamp spectra were used to establish the wavelength scale. Small adjustments derived from night-sky lines in the object frames were applied. We employed our own IDL routines to flux calibrate the data using the well-exposed continua of spectrophotometric standards (Wade & Horne 1988; Matheson et al. 2000).

An extensive series of spectra was obtained using the Inamori-Magellan Areal Camera and Spectrograph (IMACS; Dressler et al. 2011) mounted on the 6.5m Baade telescope of the Magellan Observatory. Most of these spectra are presented in our more lengthy paper, but we selected a few epochs here to demonstrate the clear detection of the broad line wings. The chosen slit width for these observations was 0''7. With the f/4 camera, we used the 300 lines per mm (lpm) grating to sample a wide wavelength range at moderate $R \simeq 500$ resolution, and the 1200 lpm grating to sample a smaller wavelength range with higher resolution of $R \simeq 6000$. The 1200 lpm grating was centered on $H\alpha$. The 2-D spectra were reduced and extracted using routines in the IMACS package in IRAF. With the f/4 camera of IMACS, the spectrum is dispersed across 4 CCD chips, so small gaps in the spectrum appear at different wavelengths depending on the grating and tilt used.

We correct all our spectra for a reddening of $E(B - V) = 1.0$ mag. This includes the minimum line-of-sight reddening in the interstellar medium (ISM) toward the Carina Nebula of $E(B - V) = 0.47$ mag (Walborn 1995; Smith 2002), plus an additional ~ 0.5 mag to account for extra extinction from dust clouds within the southern part of the Carina Nebula. This choice is explained in more detail in S18, but briefly, this reddening allows the continuum shape of various echoes to match spectral diagnostics of the temperature (Rest et al. 2012). When we deredden our spectra, the continuum shape is consistent with a temperature of about 6000 K. A different choice of $E(B - V)$ would alter the inferred continuum temperature, but would not significantly alter our conclusions about the fast ejecta, which are based on line profile shape.

¹ IRAF is distributed by the National Optical Astronomy Observatory, which is operated by the Association of Universities for Research in Astronomy, Inc., under cooperative agreement with the National Science Foundation.

² <https://github.com/cmccully/lacosmicx>

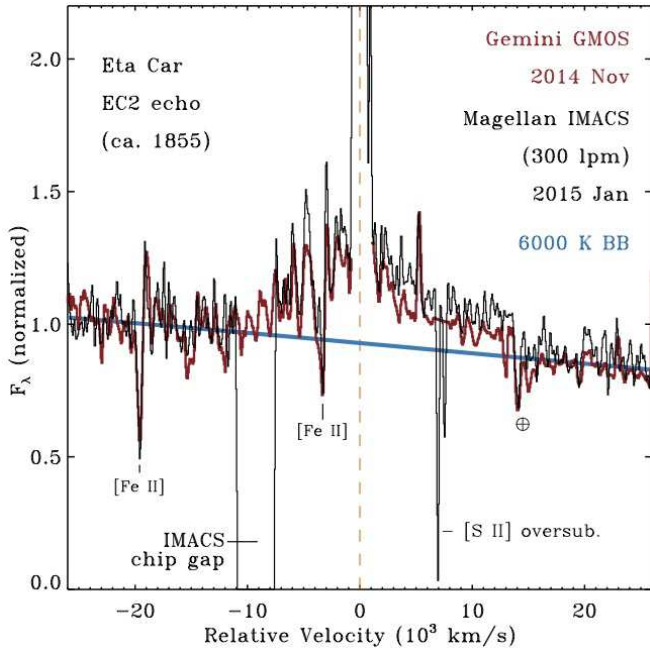


Figure 1. Low-resolution spectra of light echo EC2 corresponding to late times in the plateau phase of the eruption, showing very broad $H\alpha$ line wings. The relative Doppler shift is plotted in units of 10^3 km s^{-1} , and the broad wings of $H\alpha$ appear to extend to at least $\pm 10,000 \text{ km s}^{-1}$. The blue curve shows a 6000 K blackbody matched to the continuum.

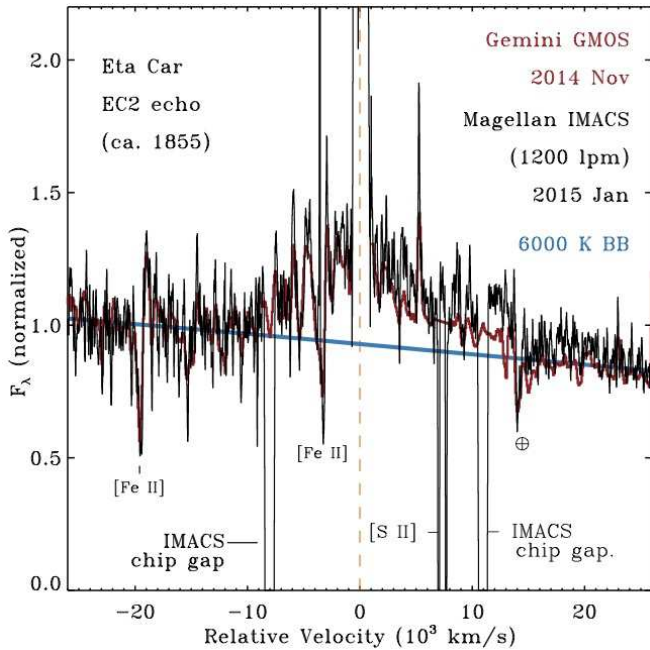


Figure 2. Same as Figure 1, but replacing the IMACS low-resolution spectrum (300 lpm grating) with a higher-resolution spectrum (1200 lpm grating) obtained on the same observing run. The same broad component appears with roughly the same strength even though a different grating is used. The same GMOS spectrum as in Figure 1 is shown again (in red) for comparison.

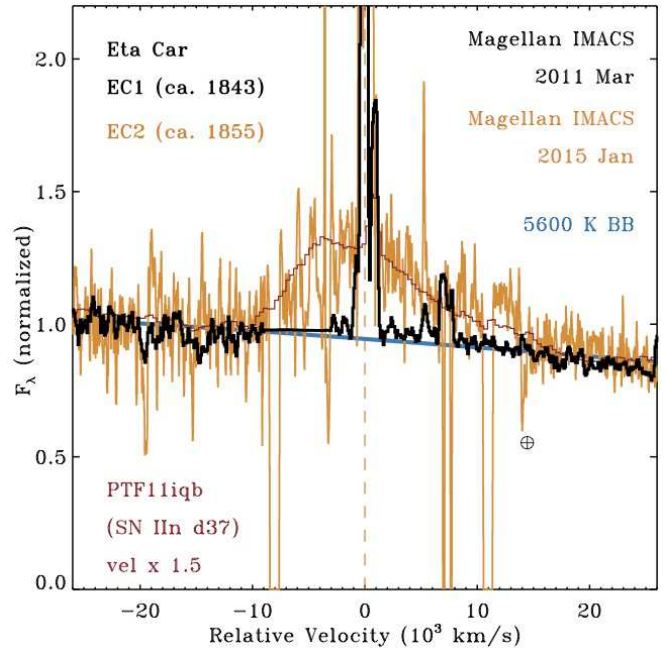


Figure 3. Similar to Figures 1 and 2, but here we plot the higher-resolution EC2 spectrum (1200 lpm grating) from Figure 2 in orange. In black, we show the spectrum of a different echo (EC1), discussed previously (Rest et al. 2012; Prieto et al. 2014), which reflects light from an early peak in the Great Eruption (1843 or 1838), also obtained with IMACS. This echo that traces an earlier phase of the eruption *does not* show the broad wings, so the fast material seems to have appeared at late phases in the eruption. Merely as an illustrative comparison, we also show the broad component in the Type IIn/II-L core-collapse supernova PTF11iqb from Smith et al. (2015), with velocities multiplied by 1.5.

3 RESULTS AND DISCUSSION

3.1 Broad $H\alpha$ Wings Trace Fast Material

Examining our low-resolution spectra of EC2, we noticed that the continuum shape in raw spectra appeared to have an unusual kink around $H\alpha$ at some epochs. After flux calibration and correcting for a modest amount of reddening of $E(B - V) = 1.0$ mag, this turned out to be low-level excess emission above the smooth continuum level. Our IMACS spectra all have chip gaps near $H\alpha$, so at first we were suspicious of a relative flux calibration offset on adjacent chips. Then in 2014 we obtained a low-resolution spectrum of EC2 with Gemini GMOS, which has no detector chip gap, and we saw the same excess. Subsequent low-resolution IMACS spectra show that this excess appeared to be growing in strength with time, more so on the red wing.

Figure 1 shows the low-resolution spectrum of EC2 near $H\alpha$, taken in 2014 with Gemini/GMOS (red-orange) and in 2015 with Magellan/IMACS (black) using the low-resolution 300 lpm grating. These epochs of the echo correspond to a date during the eruption in the mid-1850s. Broad emission wings of $H\alpha$ are seen in both spectra, and although the signal to noise in the continuum is low, the two spectra agree quite well – except that the broad emission is perhaps a bit stronger in 2015. The emission wings are interrupted by Fe II P Cygni profiles intrinsic to η Car, as well as oversubtracted

nebular [S II] emission, telluric absorption (the B band), and the IMACS chip gap.

Reducing and extracting the spectra of faint light echoes can be a bit tricky, especially in cases like η Car where we have extremely faint reflected light in the echo that is embedded in a bright H II region. To double check that the faint broad emission wings are not due to instrumental scattering from the bright nebular H α emission from the Carina Nebula H II region included in the same slit (which was, in principle, carefully subtracted with the sky emission by sampling adjacent regions along the slit), we also examined our higher resolution spectra of EC2 taken with IMACS using the 1200 lpm grating. At first glance, the broad wings were not apparent in our higher-resolution spectra, but this is because the wings are so broad that they are dispersed thinly across almost the entire sampled wavelength range and they look like continuum. In fact, the same broad wings are seen clearly in the higher resolution 1200 lpm grating IMACS spectra when they are plotted on the same intensity scale as the low-resolution spectra. Figure 2 is the same as Figure 1, except that we replaced the 300 lpm IMACS spectrum with the 1200 lpm IMACS spectrum obtained on the same night. The two IMACS spectra are consistent within the limitations of signal to noise. Since we see the same broad emission wings in two different instruments on two different telescopes, and also with two different gratings in the same instrument, this broad emission must be real and intrinsic to η Carinae's light echo.

These broad emission wings are not due to some other source of broad emission within the Carina Nebula, because the broad wings are absent in spectra of other (EC1) light echoes from η Car in the same part of the sky (about 2' away), which trace earlier peaks (1843 or before) in the Great Eruption (Rest et al. 2012; Prieto et al. 2014). A spectrum of one of these earlier EC1 echoes (also obtained with the IMACS spectrograph on Magellan) is shown in Figure 3 (thick black line), as compared to the same 1200 lpm spectrum of EC2 (orange). *Clearly the broad component is absent or much weaker in the EC1 echo that corresponds to an earlier phase of the eruption.* This confirms that the broad emission wings appeared relatively late in the Great Eruption. Even in our spectra of this new EC2 echo, the broad wings are somewhat weaker in our earliest spectra in 2011/2012, but strengthen through 2014 and 2015 until the present. From the adopted time delay for the echo of ~ 160 years, this suggests that the broad emission wings became prominent in the mid-1850s. It is interesting that the emergence of fast material in spectra occurs shortly after the ejection date of 1847.1 (± 0.8 yr) deduced from proper motions of the Homunculus (Smith 2017). The broad emission wings are also absent in the extracted spectrum of a field star that was included in the same IMACS slit aperture about an arcminute away from EC2 (Figure 4), confirming that they are not instrumental.

The broad H α emission wings in Figures 1 and 2 are unprecedented for an LBV eruption. The blue wing extends to $-10,000$ km s $^{-1}$. The red wing extends past $+10,000$ km s $^{-1}$, to at least $+14,000$. It is difficult to determine the farthest extent of the red wing due to the telluric B band absorption (marked by \oplus in the figures) overlapping that part of the line profile. Figure 4 presents a correction for the telluric absorption on the red wing of H α . Although we did not obtain

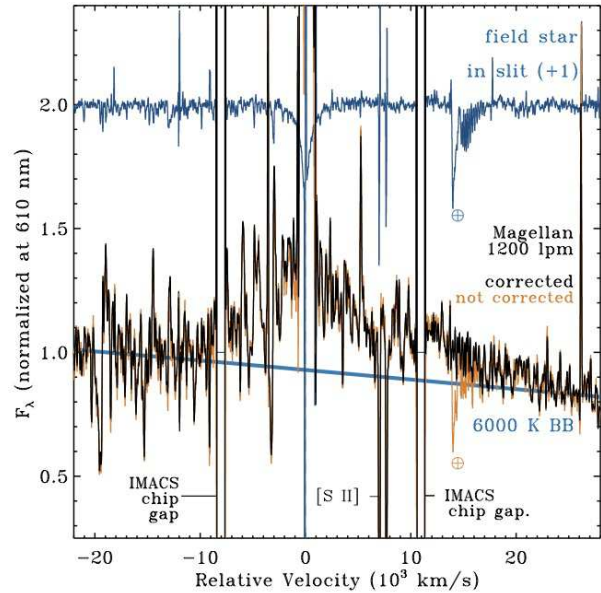


Figure 4. The effects of telluric absorption on the broad redshifted emission wing of H α in the EC2 spectrum. The orange tracing (with no correction for telluric absorption) is the same IMACS 1200 lpm spectrum of EC2 as in Figure 2. The black tracing shows this same H α line profile after correcting for telluric absorption by the B-band (marked by \oplus). The blue tracing is the spectrum of a field star that was included about one arcminute away in the same slit, in the same exposures as the observations of EC2. This is not a proper telluric standard, and the strong H α absorption corrupts the H α emission of EC2 at low velocities, but it is useful to correct for the telluric absorption of the B-band on the red wing of the line. After correcting for telluric absorption (black) the red wing drops smoothly from $+12,000$ km s $^{-1}$ to beyond $+20,000$ km s $^{-1}$. Exactly how much farther the red wings extends beyond $+20,000$ km s $^{-1}$ depends on the choice of the admittedly noisy continuum level.

an appropriate set of telluric standard star observations to correct the full spectra, one of our slit positions using the IMACS 1200 lpm grating to observe EC2 also included a bright field star in the same slit about an arcminute away. This star appears to be a late B-type or early A-type star, so the H α absorption intrinsic to this star is fairly strong and corrupts the telluric correction at low velocities (± 1500 km/s). However, the continuum in the vicinity of the atmospheric B-band is smooth and provides a suitable way to correct for the telluric absorption on the red wing of H α . The extracted spectrum of this field star is shown in blue in Figure 4. We divided the observed spectrum of EC2 by this field star to correct for the telluric B-band absorption. Figure 4 shows the IMACS 1200 lpm spectrum before (orange) and after (black) correction of the telluric absorption. After correcting for telluric absorption in this way, the resulting line profile shows that the broad wings are asymmetric, extending farther on the red side out to at least $+20,000$ km s $^{-1}$. Both the red and blue wings are extreme compared to the relatively narrow core of the H α line, which has a width of about ± 600 km s $^{-1}$.

Narrow line cores can have broad electron-scattering wings, as is commonly seen in dense stellar winds and early spectra of SNe II α , and these wings can extend to larger ve-

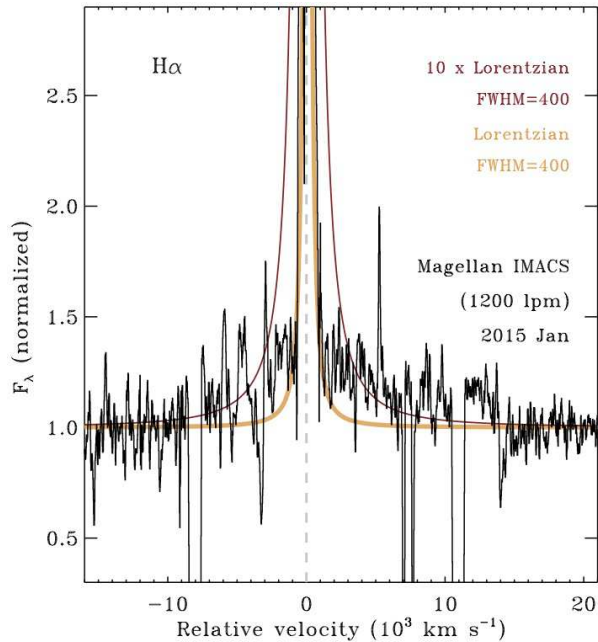


Figure 5. The observed broad wings compared to Lorentzian profiles expected for electron scattering wings. The black spectrum is the same Magellan/IMACS 1200 lpm spectrum of EC2 in Figure 2, normalized to the red continuum. If the broad wings were caused by electron scattering, they should follow a roughly symmetric Lorentzian profile. The width of any such profile is restricted by the width of the narrow line core at about 1.5 times the continuum level in this plot. The thick orange curve shows a Lorentzian profile with $\text{FWHM} = 400 \text{ km s}^{-1}$ that roughly approximates the width at the base of the central line core, and it vastly underpredicts the flux of the broad wings and has the wrong shape. The thinner red curve is the same Lorentzian multiplied by a factor of 10 in flux above the continuum; this can account for the flux in the very broad wings, but then the Lorentzian profile vastly overpredicts the flux at around $\pm 1500 \text{ km s}^{-1}$.

locities than the true kinematic speed of ejecta. Indeed, the present-day wind spectrum of η Car shows an $\text{H}\alpha$ profile with electron-scattering wings that extend beyond $\pm 1000 \text{ km s}^{-1}$ (Hillier et al. 2006; Smith et al. 2003a), even though the wind speed is only about $400\text{--}500 \text{ km s}^{-1}$. However, electron scattering cannot explain the broad emission wings seen in spectra of EC2, because they are too broad and have the wrong shape. With a characteristic temperature around 6000 K , scattering off thermal electrons will produce wings with a width of only about $\pm 500\text{--}1000 \text{ km s}^{-1}$. Even in the early phases of SNe II_n when the temperatures might be $20,000 \text{ K}$ (as in η Car’s present-day wind), the electron scattering wings only have widths (FWHM) of typically $\pm 1500 \text{ km s}^{-1}$. Moreover, the broad wings seen in Figures 1 and 2 do not have the characteristic symmetric Lorentzian profiles expected for electron scattering.

Figure 5 compares the observed $\text{H}\alpha$ profile to Lorentzian profile shapes. A Lorentzian profile is expected if the wings are produced primarily by electron scattering, as is seen in early observations and models of SNe II_n (Chugai 2001; Smith 2008; Dessart et al. 2016). It is clear that a Lorentzian profile cannot match both the broad wings and the narrow width at the base of the central narrow emission line component in η Car’s echo. The thick orange Lorentzian, with

$\text{FWHM} = 400 \text{ km s}^{-1}$, roughly matches the width at the base of the narrow component (note that this is not a good approximation of the shape of the narrow component, which is somewhat irregular and asymmetric, but it does agree with the widest point at the base of the narrow component). However, when this profile is extrapolated to high velocities, it vastly underpredicts the observed flux in the broad wings. If we increase the flux of this Lorentzian (thin red profile) so that it can produce the observed flux in the broad wings at $\pm 5000 \text{ km s}^{-1}$, we find that it vastly overpredicts the flux at lower speeds around $1000\text{--}2000 \text{ km s}^{-1}$, so that the base of the narrow component is much broader than observed. This Lorentzian profile also vastly overpredicts the total $\text{H}\alpha$ line flux. We conclude that electron scattering due to high optical depths in a slower outflow cannot explain the broad wings we report in light echoes of η Car.

Instead, the broad emission must trace fast ejecta, separate from the slower material emitting the narrower line core. The observed broad component has a peak shifted to the blue, with a very long red tail. This asymmetry might be due to partial P Cygni absorption of the broad blue emission wing. Similar broad profiles with blue peaks and extended red wings are sometimes seen in fast ejecta from SNe; an example from the SN II-L/II_n PTF11iqb (Smith et al. 2015) is shown in red in Figure 3. In this comparison (meant to illustrate a possibly similar line-profile shape), we have multiplied the outflow velocity of PTF11iqb by a factor of 1.5 for comparison, because the wings in η Car’s echo are actually broader than in this core-collapse SN.

3.2 Implications

The broad wings of $\text{H}\alpha$ seen in light echo spectroscopy of η Car are remarkable, and are reminiscent of SN ejecta speeds. To our knowledge, these are the fastest speeds yet seen in any non-terminal massive star eruption. The fastest speeds seen from the central star (as fast as -2000 km s^{-1}) are only seen in absorption at certain phases, and have been attributed to the companion’s wind as it shocks the primary star’s wind along our line of sight (Groh et al. 2010).

The broad emission wings that we report are faint, and only trace a fraction of the total outflowing matter. It is not necessarily an insignificant fraction, though; the integrated flux of the broad component is about $1/3$ of the total $\text{H}\alpha$ line flux. It appears relatively faint because it is spread across such a wide wavelength range. The brighter narrow emission line core of $\text{H}\alpha$ shows widths around $500\text{--}600 \text{ km s}^{-1}$, more in line with the bulk outflow velocity in the Homunculus nebula. Even if it is only tracing a portion of the mass, an outflow speed of $\sim 10,000 \text{ km s}^{-1}$ or more is surprising, and has important implications for understanding the basic nature of η Car’s eruption and its energy budget. There are a few key considerations:

1. The outflow speeds of $10,000\text{--}20,000 \text{ km s}^{-1}$ indicated by the broad $\text{H}\alpha$ wings are two orders of magnitude faster than the escape speed from a warm supergiant. For η Car in its cool, bloated eruption state (a radius of a few hundred R_{\odot} ; Smith 2011), we would expect a dense, super-Eddington wind to have a speed on the order of the escape velocity or less (Owocki et al. 2004; van Marle et al. 2008, 2009; Smith 2013), or about 200 km s^{-1} . This is indeed the speed observed in light echoes from the early

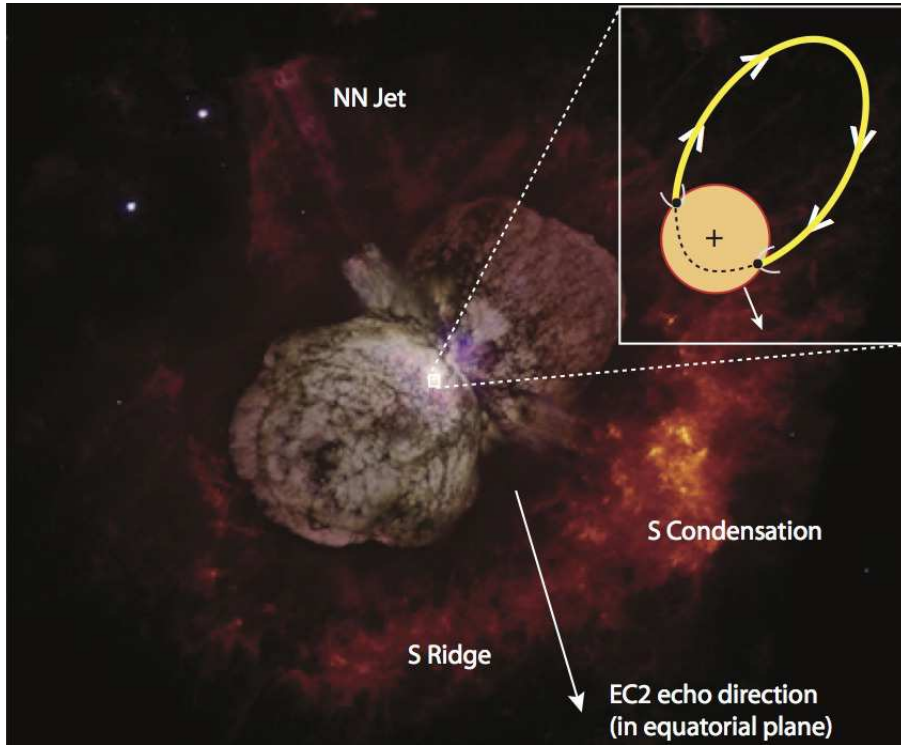


Figure 6. A color *HST*/WFPC2 image of η Car and its ejecta (N. Smith/U. Arizona and NASA) showing the direction from which the EC2 light echo views η Car (this is in or near the equatorial plane). The diagram inset at the upper right shows the orbital orientation of the eccentric binary system adapted from Madura et al. (2012), but with the primary star (orange) bloated to a large radius appropriate for its temperature and luminosity in the eruption, adopted from Smith (2011). The arrows show the direction of motion of the secondary, the two black dots are the points of ingress and egress, and the dashed curve is the part of the orbit when the secondary is inside the primary star's bloated envelope. The directions of ingress and egress are curiously similar to the trajectories of the S Condensation and NN Jet, respectively.

1840s peaks in the eruption (Rest et al. 2012; Prieto et al. 2014), and the speed observed in spectra of the 1890 event (Walborn & Liller 1977). The broad lines that developed in η Car's echo indicate that something besides a steady wind is at work. The extremely fast speeds are also ~ 10 times faster than the escape speed from an O-type star or Wolf-Rayet star, which might correspond to η Car's companion star that survives today. Instead, such high speeds are reminiscent of outflows from disks around compact objects or fast shock-accelerated ejecta in SN explosions. The relatively late emergence of the fast material may be consistent with the suggestion (Smith 2013) that a blast wave would accelerate as it encountered a steep drop in density upon existing the outer boundary of a dense CSM shell, or it may be indicative of the fastest ejecta getting excited near a reverse shock during later CSM interaction.

2. The fact that this echo reflects light seen from a vantage point near the equatorial plane of the Homunculus is critical to interpreting the broad emission. Fast outflow velocities could be interpreted as evidence of a jet that arises when material is accreted onto a companion star (Kashi & Soker 2009; Soker 2001, 2004; Tsebrenko & Soker 2013). In such models, it has been proposed that a main-sequence O-type star accretes matter at periastron passages and blows bipolar jets that shape the Homunculus Nebula. However, it is difficult to see how such a jet could achieve speeds well in excess of the escape speed from an

O-type dwarf; the observed speeds might be more indicative of accretion-driven jets from a compact object companion. More importantly, however, even this jet scenario would not result in such fast outflow speeds in the *equatorial* direction, because in such models, a highly collimated polar jet is invoked to shape the bipolar Homunculus lobes. That polar axis is perpendicular to the viewing angle of the echo discussed here. Instead, the broad wings in echoes seen from low latitudes point to something more like a wide-angle explosion.

3. The fast material indicated by the broad wings in the EC2 echo may be related to fast nebular material seen today in the Outer Ejecta of η Car. Most of the bright material in the Outer Ejecta is composed of dense nitrogen-rich condensations moving at speeds of several hundred km s^{-1} (Davidson et al. 1982; Kiminki et al. 2016; Mehner et al. 2016; Smith & Morse 2004; Smith 2008; Walborn 1976; Weis et al. 2001; Weis 2012). Some features seen in images are moving at $\sim 10^3 \text{ km s}^{-1}$ (Smith & Morse 2004; Weis et al. 2001; Weis 2012). However, the fastest material can only be seen in spectra (Doppler shifted out of narrow-band imaging filters); it appears to be concentrated in polar directions, and is expanding away from the star at around $5,000 \text{ km s}^{-1}$ with a likely origin during the Great Eruption (Smith 2008). It seems probable that the fastest nebular material in the Outer Ejecta seen today may be a counterpart to the fast material seen in light echo spectra.

If an explosion produced ejecta with a range of speeds up to $20,000 \text{ km s}^{-1}$, then the fastest of this material would have already crashed into the reverse shock, and has therefore given up its kinetic energy to power the X-ray shell around η Car (Seward et al. 2001; Smith & Morse 2004). Material expanding toward the poles at $\sim 5,000 \text{ km s}^{-1}$ or less is still in free expansion because it has not yet reached the reverse shock, consistent with its observed location inside the X-ray shell (Smith 2008).

Since the EC2 echo discussed here views η Car from a latitude near the equator, it is interesting to speculate about implications for the equatorial ejecta around the Homunculus and connections to the central binary system. The brightest feature in the Outer Ejecta of η Car is the so-called ‘‘S Condensation’’ (part of the ‘‘S Ridge’’), located to the S/SW from the star and redshifted (Walborn 1976; Davidson et al. 1982; Kiminki et al. 2016; Smith & Morse 2004). Its trajectory of ejection from the star is not far from the viewing angle of the echo discussed in this work (see Figure 6). Is the S Condensation related to the fast material observed in light echo spectra? Today the S Condensation is much slower (expanding at a few hundred km s^{-1}), but the S Condensation we see today could be the end product of a small mass of very fast ejecta from the Great Eruption that swept up and shocked much denser and slower CSM in the equator. Proper motions of material in the S Ridge yield ejection dates several decades before the Great Eruption (Kiminki et al. 2016; Morse et al. 2001), consistent with older and slower CSM that may have been accelerated when hit by the fast ejecta.

Perhaps even more interesting (and more speculative) is a possible connection to violent binary interaction during the eruption itself. Smith (2011) pointed out that with the emitting radius required to achieve the observed luminosity during the lead-up to the eruption, the bloated primary star’s effective photosphere was actually bigger than the separation of the two stars at periastron in the current binary system — this means that the secondary star plunged into the extended envelope of the primary (or some extended common envelope around the system) and came out the other side, doing so multiple times. The orientation of the present-day eccentric binary system is aligned with the equatorial plane of the Homunculus, and has the secondary star orbiting clockwise on the sky, with periastron in the direction away from Earth (Madura et al. 2012). With this geometry (shown in Figure 6), the point of ingress when the secondary star collided with the bloated envelope is on the S/SW side of the star, such that the direction toward the echo is similar to the point of ingress. In other words — *the echo is situated favorably to have viewed the secondary star plunging into the bloated primary star’s envelope.* (Of course, the central ‘‘primary star’’ here may have been a close binary in the midst of a merger event surrounded by a common envelope.) Similarly, the direction of egress from the bloated envelope seems well aligned with the trajectory of the NN Jet (Figure 6). Some speculation is required here, since to our knowledge there have been no 3-D hydrodynamic numerical simulations to explore such a scenario of two massive stars colliding in an eccentric binary with a bloated primary. One can imagine a small mass of high velocity ejecta accelerated by the ensuing splash, which may far exceed the orbital speed of the secondary, or a small amount of shock accelerated ejecta escaping through a chim-

ney formed by the wake of the orbiting companion. This violent collision may have had something to do with the fast ejecta revealed in the spectra of light echoes reported here, and it may have ejected fast material preferentially in the directions of the S Condensation and NN Jet.

3.3 SN 2009ip

There are also interesting connections to extragalactic objects. Most LBVs and SN impostors show $\text{H}\alpha$ line widths that indicate bulk outflow speeds from a few hundred up to 1000 km s^{-1} (Smith et al. 2011), like the majority of the mass flux in η Car. Similar speeds are seen in the CSM of Type II n supernovae (see Smith 2014).

One remarkable exception is the case of SN 2009ip, which was a luminous and eruptive LBV-like star observed in eruption in 2009 (Smith et al. 2010; Foley et al. 2011), but which then exploded as a SN a few years later (Mauerhan et al. 2013). Spectra of pre-SN outbursts showed some very fast material in SN 2009ip with speeds as high as $7,000\text{--}10,000 \text{ km s}^{-1}$ (Smith et al. 2010; Foley et al. 2011; Pastorello et al. 2013). An important point, though, is that this fast material was only seen in absorption along the line of sight, whereas the main emission line core was relatively narrow, indicating outflow speeds for the bulk of the material of 600 km s^{-1} . This situation, with the bulk of the mass moving more slowly and a fraction of the ejecta accelerated to very high speeds, is strikingly similar to what we see in echoes of η Car and in its fast Outer Ejecta (Smith 2008). This provides yet another empirical link between LBVs and the progenitors of some SNe II n , and provides interesting clues to the possibly similar mechanisms of pre-SN eruptive mass loss. The existence of this fast ejecta is a strong constraint for any physical model of the eruption mechanism.

4 SUMMARY AND CONCLUSIONS

This paper presents spectra of light echoes from η Carinae that correspond to the time period of the main plateau of the eruption during the late 1840s through the 1850s. The full spectral evolution, photometry, and other details of this echo will be discussed in a forthcoming paper (S18). Here we focus on one important aspect that is significant on its own, which is the discovery of extremely broad emission wings of $\text{H}\alpha$ that represent the fastest material ever detected in an LBV-like eruption. The main results from this work are summarized as follows.

1. In addition to a relatively narrow (600 km s^{-1}) line core, $\text{H}\alpha$ displays extremely broad wings in emission, reaching to approximately $-10,000 \text{ km s}^{-1}$ to the blue and $+20,000 \text{ km s}^{-1}$ or more on the red wing.

2. We demonstrate that the broad wings are not instrumental. They are not present in a nearby field star included in the same slit, and moreover, the same broad wings are seen in spectra obtained with different instruments on different telescopes as well as two different gratings on the same spectrograph. The strength of the broad wings changes with time, and the broad emission is not seen in a different echo that traces earlier epoch in the eruption seen from a similar direction. Correcting for the telluric B-band absorption, the red wing clearly extends to $+20,000 \text{ km s}^{-1}$ or more.

3. The shape of the broad wings is inconsistent with electron scattering wings, and we argue that the broad emission must trace Doppler shifts from bulk expansion velocities. Therefore, these are the highest outflow speeds discovered yet in an LBV or any non-terminal eruptive transient.

4. The high velocities are too fast for any previously conceived escape velocity in the system, but similar to outflow speeds from accreting compact objects or expansion speeds of SN ejecta. The expanding material probably does not arise in a steady wind, but instead likely indicates a shock-accelerated outflow.

5. The broad wings are seen in echo spectra that view η Car from the equator, so these high speeds are probably not indicative of a polar jet (even one from a compact object). The high speeds in echoes seen from the equator combined with fast polar speeds in the Outer Ejecta seen today (Smith 2008) suggest a wide-angle explosion rather than a highly collimated jet.

6. The viewing angle of this echo could be special, however, since it is looking from a similar direction as the “S Condensation” in the Outer Ejecta. This is also a special direction in the present day binary system, since it is situated preferably to view the wide companion plunge into a putative common envelope, for example (see text).

7. Regardless of the physical interpretation, the dual presence of fast and slow speeds (10,000-20,000 km s⁻¹ and 600-1000 km s⁻¹, respectively) point to CSM interaction at work in the eruption. They are also similar to slow and high velocities seen in spectra of the eruptive progenitor of SN 2009ip. Therefore, the high velocities in η Car provide yet another interesting possible link between LBVs and SNe II_n.

ACKNOWLEDGEMENTS

We thank an anonymous referee for a careful reading of the manuscript and constructive comments. We acknowledge contributions of additional collaborators who helped with imaging observations to discover and monitor light echoes, as well as for discussions and contributions to proposals for telescope time for this and related projects: the Carnegie Supernova Project, Alejandro Clocchiatti, Steve Margheim, Doug Welch, and Nolan Walborn. In particular, Nolan Walborn provided helpful comments on the manuscript just weeks before he passed away, which occurred while this paper was under review. His contributions to massive star research have been tremendous, and his unique insight will be sorely missed.

NS's research on Eta Carinae's light echoes and related LBV-like eruptions received support from NSF grants AST-1312221 and AST-1515559. Support for JLP is provided in part by FONDECYT through the grant 1151445 and by the Ministry of Economy, Development, and Tourism's Millennium Science Initiative through grant IC120009, awarded to The Millennium Institute of Astrophysics, MAS. DJJ gratefully acknowledges support from the National Science Foundation, award AST-1440254.

This paper includes data gathered with the 6.5m Magellan Telescopes located at Las Campanas Observatory, Chile. Based, in part, on observations obtained at the Gemini Observatory, which is operated by the Association of Universities for Research in Astronomy, Inc., under a cooperative agreement with the NSF on behalf of the Gemini partnership: the National Science Foundation (United States), the National Research Council (Canada), CONICYT (Chile), Ministerio de Ciencia, Tecnología e Innovación Productiva (Argentina), and Ministério da Ciência, Tecnologia e Inovação (Brazil) (Program GS-2014B-Q-24).

REFERENCES

Abbott DC. 1982, ApJ 259, 282
 Castor JI, Abbott DC, Klein RI. 1975, ApJ 195, 157
 Chugai NN. 2001, MNRAS, 326, 1448
 Corcoran MF, Ishibashi K, Swank JH, Petre R. 2001, ApJ, 547, 1042
 Couderc P. 1939, Annales d'Astrophysique, 2, 271
 Davidson K. 1987, ApJ, 317, 760

Davidson K., Walborn N. R., Gull T. R., 1982, ApJ, 254, L47
 Dessart L, Livne E, Waldman R. 2010, MNRAS, 405, 2113
 Dessart L, Hillier DJ, Livne E, Waldman R. 2016, MNRAS, 458, 2029
 Dressler A, Bigelow B, Hare T, et al. 2011, PASP, 123, 288
 Foley R.J., Berger E., Fox O., et al. 2011, ApJ, 732, 32
 Fuller J. 2017, arXiv:1704.08696
 Gallagher J. S., 1989, in Davidson K., Moffat A. F. J., Lamers H. J. G. L. M., eds, Astrophysics and Space Science Library, Vol. 157. IAU Colloq. 113: Physics of Luminous Blue Variables. Kluwer, Dordrecht, p. 185
 Gal-Yam A, Leonard DC. 2009, Nature, 458, 865
 Glazebrook K, Bland-Hawthorn J. 2001, PASP, 113, 197
 Groh JH, Nielson KE, Damiani A, et al. 2010, A&A, 517, A9
 Groh JS, Meynet G, Ekström S. 2013, A&A, 550, L7
 Groh JS. 2014, A&A, 572, L11
 Guzik JA, Lovekin CC. 2012, Astron. Rev., 7, c13
 Harpaz A, Soker N. 2009, New Astr., 14, 539
 Hillier, D. J., Gull, T., Nielsen, K., et al. 2006, ApJ, 642, 1098
 Hook I, et al. 2002, SPIE, 4841
 Horne K. 1986, PASP, 98, 609
 Justham S, Podsiadlowski P, Vink JS. 2014, ApJ, 796, 121
 Kashi A, Soker N. 2009, New Astron., 14, 11
 Kiminki MM, Reiter M, Smith N. 2016, MNRAS, 463, 845
 Kotak R, Vink JS. 2006, A&A, 460, L5
 Lamers HJGLM, Snow TP, Lindholm DM. 1995, ApJ 455, 269
 Madura T.I., et al. 2012, MNRAS, 420, 2064
 Matheson, T., Filippenko, A. V., Ho, L. C., Barth, A. J., & Leonard, D. C. 2000, AJ, 120, 1499
 Mauerhan J.C., Smith N., Filippenko, A.V., et al. 2013, MNRAS, 430, 1801
 Mehner A, et al. 2016, A&A, 595, A120
 Morse J. A., Kellogg J. R., Bally J., Davidson K., Balick B., Ebbets D., 2001, ApJ, 548, L207
 Owocki SP, Gayley KG. 1997, in Luminous Blue Variables: Massive Stars in Transition, ASP Conf. Ser. 120, ed. A. Nota & H. Lamers (San Francisco: ASP), 121
 Owocki S. P., Shaviv N. J. 2016, MNRAS, 462, 345
 Owocki S. P., Gayley K. G., Shaviv N. J., 2004, ApJ, 616, 525
 Owocki SP, Townsend RHD, Quataert E. 2017, in press
 Parkin ER, Pittard JM, Corcoran MF, Hamaguchi K. 2011, ApJ, 726, 105
 Pastorello A. et al., 2013, ApJ, 767, 1
 Pauldrach AWA, Puls J. 1990, A&A 237, 409
 Pauldrach AWA, Puls J, Kudritzki RP. 1986, A&A 164, 86
 Piro A. 2011, ApJ, 738, L5
 Pittard JM, Corcoran MF. 2002, A&A, 383, 636
 Portegies Zwart S. F., van den Heuvel E. P. J., 2016, MNRAS, 456, 3401
 Prieto JL, et al. 2014, ApJ, 787, 8
 Quataert E, Shiode J. 2012, MNRAS, 423, L92
 Quataert E, Fernandez R, Kasen D, Klion H, Paxton B. 2016, MNRAS, 458, 1214
 Rest A, et al. 2012, Nature, 482, 375
 Rest, A., Stubbins, C., Becker, A. C., et al. 2005a, ApJ, 634, 1103
 Rest, A., Suntzeff, N. B., Olsen, K., et al. 2005b, Nature, 438, 1132
 Rest, A., Welch, D. L., Suntzeff, N. B., et al. 2008, ApJL, 681, L81
 Ro S, Matzner CD. 2017, ApJ, 849, 9
 Russell CMP, Corcoran MF, Hamaguchi K, Madura TI, Owocki SP, Hillier DJ. 2016, MNRAS, 458, 2275
 Seward, F. D., Butt, Y. M., Karovska, M., Prestwich, A., Schlegel, E. M., Corcoran, M. F. 2001, ApJ, 553, 832
 Shiode JH, Quataert E. 2014, ApJ, 780, 96
 Smith N. 2002, MNRAS, 331, 7
 Smith N. 2006, MNRAS, 364, 1151
 Smith N. 2007, AJ, 133, 1034
 Smith N. 2008, Nature, 455, 201
 Smith N. 2011, MNRAS, 415, 2020
 Smith N. 2013, MNRAS, 429, 2366
 Smith N. 2014, ARAA, 52, 487
 Smith N. 2017, MNRAS, 471, 4465
 Smith N, Arnett WD. 2014, ApJ, 785, 82
 Smith N, Frew D. 2011, MNRAS, 415, 2009
 Smith N, McCray R. 2007, ApJ, 671, L17
 Smith N, Morse JA. 2004, ApJ, 605, 854
 Smith N, Owocki SP, 2006, ApJ, 645, L45
 Smith N, Davidson K, Gull TR, Ishibashi K, Hillier DJ. 2003a, ApJ, 586, 432
 Smith N., Gehrz R. D., Hinz P. M., Hoffmann W. F., Hora J. L., Mamajek E. E., Meyer M. R., 2003b, AJ, 125, 1458
 Smith N, Li W, Foley RJ, et al. 2007, ApJ, 666, 1116
 Smith N, Chornock R, Li W, et al. 2008, ApJ, 686, 467
 Smith N., Miller A., Li W., et al. 2010, AJ, 139, 1451
 Smith N., et al. 2011, MNRAS, 415, 773
 Smith N., et al. 2015, MNRAS, 449, 1876
 Smith N., et al. 2016a, MNRAS, 455, 3546
 Smith N., et al. 2016b, MNRAS, 458, 950
 Smith N., et al. 2018, MNRAS, submitted
 Soker N, 2001, MNRAS, 325, 584

- Soker N. 2004, ApJ, 612, 1060
Trundle C., Kotak R., Vink J. S., Meikle W. P. S., 2008, A&A, 483, L47
Tsebrenko D, Soker N. 2013, ApJ, 777, L35
van Dokkum, P. G. 2001, PASP, 113, 1420
Van Dyk S. D., Matheson T., 2012, in Humphreys R. M., Davidson K., eds, *Eta Carinae and the Supernova Impostors*. Springer, Berlin, 249
van Marle AJ, Owocki SP, Shaviv NJ. 2008, MNRAS, 389, 1353
van Marle AJ, Owocki SP, Shaviv NJ. 2009, MNRAS, 394, 595
Vink JS, de Koter A, Lamers HJGLM. 1999, A&A, 350, 181
Wade, R. A., & Horne, K. D. 1988, ApJ, 324, 411
Walborn N. R., 1976, ApJ, 204, L17
Walborn NR. 1995, Rev. Mexicana Astron. Astrofis. Ser. Conf., 2, 51
Walborn NR, Liller MH. 1977, ApJ, 211, 181
Weis K., 2012, in Davidson K., Humphreys R. M., eds, *Astrophysics and Space Science Library*, Vol. 384. *Astrophysics and Space Science Library*. p. 171
Weis K., Duschl W. J., Bomans D. J., 2001, A&A, 367, 566
Woosley SE. 2017, ApJ, 836, 244